

## Vector Stochastic Properties of A Fiber Raman Amplifier

Vladimir L. Kalashnikov<sup>1,2</sup>, Sergey V. Sergeev<sup>1</sup>

<sup>1</sup>Aston Institute of Photonic Technologies, Aston University, Aston Triangle, Birmingham, B4 7ET, UK

<sup>2</sup>Institute of Photonics, Vienna University of Technology, Vienna, A-1040, Austria  
(E-mail: vladimir.kalashnikov@tuwien.ac.at)

**Abstract.** Direct numerical simulations of nonlinear vector light evolution in a Raman fiber amplifier with a random birefringence were performed in both Stokes and Jones representations. The Jones representation allows separating a stochastic part governed by material birefringence from a vector field dynamics governed by generalized vector nonlinear Schrödinger equation. The material part can be calculated independently from a system of stochastic ordinary differential equations and represented in the form of a universal library of stochastic coefficients for any type of dynamic vector partial differential equations. This approach demonstrated a resonance stochastization of the signal state of polarization within diapasons of the polarization mode dispersion parameter  $\approx 0.02$  ps/km<sup>1/2</sup> and the fiber length  $\approx 6$  km. The effect can be interpreted as a simultaneous manifestation of stochastic anti-resonance and Raman nonlinearity, i.e. depletion of the pump by a signal with intra-fiber propagation. Pump-signal noise transfer is maximum near stochastic anti-resonance, but it does not vanish and can even grow with a decrease of the polarization mode dispersion. It was found, that the growth of signal power, i.e. enhancement of pump depletion, suppresses signal stochastization. Two multi-scale averaging analytical techniques were developed. They agree perfectly with numerical results in the limits of small and large propagation lengths as well as for arbitrary fiber length in the case of small polarization mode dispersions. The obtained results can be usable for both design of new generation of high-speed telecommunication systems and development of new multi-scale averaging mathematical techniques.

**Keywords:** Stochastic modeling, Multi-scale averaging techniques, Vector Raman amplification, Stochastic anti-resonance, Pump-signal noise transfer.

### 1 Introduction

Raman amplification became an efficient tool for high-speed telecommunication due to its high efficiency and the possibility to provide homogeneous amplification within broad spectral range and, thereby, to increase the number of communication channels substantially (see C. Headley & G.P. Agrawal [1]). The characteristic feature of Raman amplification is its vector nature that is dependence on relative states of polarization (SOP) of pump and signal. Both pump and signal propagate through a fiber with inherent birefringence caused, for instance, by noncircularity of fiber core or mechanical stress, which are randomly distributed along a fiber. Their combined effect on the evolution of pump and signal SOPs is described by so-called polarization mode dispersion



parameter (PMD)  $D_p \equiv 2\lambda_s \sqrt{L_c} / cL_{bs}$ , where  $\lambda_s$  is a signal wavelength,  $c$  is a light speed,  $L_{bs}$  is a signal polarization beat length and  $L_c$  is a coherence length of random birefringence (see A. Galtarossa and C.R. Menyuk [2]). If the scales of regular and random birefringence differ substantially so that  $L_{bs} \gg L_c$ , pump SOP pulls signal one after sufficiently long propagation (the so-called phenomenon of “polarization pulling” or “trapping,” V.V. Kozlov *et al.* [3]). In this regime, the signal SOP fluctuates slightly relatively the pump one (see V.L. Kalashnikov *et al.* [4]). Such a limit, when a fiber acts as an effective polarizer relatively pump SOP, will be called as the “Manakov limit” thereafter. Opposite limit of  $L_c \gg L_{bs}$  corresponds to complete decorrelation of signal and pump SOPs due to their fast relative rotation so that a fiber acts as an isotropic medium (so-called “diffusion limit,” V.V. Kozlov *et al.* [3]). Most nontrivial regime corresponds to  $L_c \approx L_{bs}$  and manifests itself in abrupt stochastization of the signal SOP evolution. It is so-called “stochastic anti-resonance” (SAR) regime (V.L. Kalashnikov *et al.* [4]).

In this work, we present the results of a systematic investigation of stochastic and noise properties of a fiber Raman amplifier in dependence on PMD and a fiber length  $L$  with taking into account nonlinearity in the form of pump depletion. New multi-scale averaging techniques are presented and compared with the numerical results. The latter are based on an original approach dividing the initial system of stochastic evolutionary equations (PDEs in general case) for pump and signal in Jones representation on the systems of evolutionary PDEs with stochastic birefringence coefficients for pump and signal, and the independent system of stochastic ODEs for the birefringence coefficients. These coefficients are calculated on one occasion only and can be used for a multitude of dynamical problems, i.e. realization of a fiber Raman amplifiers. Finally, we touch on problem pump-signal noise transfer.

## 2 Model and Methods

We base our analysis on the Manakov PMD equations in Jones representation without taking in account group-delay, group-velocity dispersion, and Kerr nonlinearity. These assumptions are quite valid for the pump powers  $P_{in} \leq 1$  W and the propagation lengths  $L < 100$  km. The corresponding system of equations for a signal  $|A_s\rangle$  and a pump  $|A_p\rangle$  taking into account stochastic birefringence and pump depletion is (C.R. Menyuk and B.S. Marks [5]; and V.L. Kalashnikov and S.V. Sergeyev [6]):

$$\begin{aligned}\frac{d|A_s\rangle}{dz} &= \frac{g_R}{2}|A_p\rangle\langle A_p|A_s\rangle - \alpha_s|A_s\rangle + \frac{i\pi}{L_{bs}}(\sigma_3 \cos \theta + \sigma_1 \sin \theta)|A_s\rangle, \\ \frac{d|A_p\rangle}{dz} &= -\frac{g_R\lambda_s}{2\lambda_p}|A_s\rangle\langle A_s|A_p\rangle - \alpha_p|A_p\rangle + \frac{i\pi}{L_{bp}}(\sigma_3 \cos \theta + \sigma_1 \sin \theta)|A_p\rangle, \\ d\theta(z) &= \ell(z) \circ dz,\end{aligned}\quad (1)$$

where  $z$  is a propagation coordinate,  $g_R$  is a Raman gain coefficient,  $\lambda_p$  is a pump wavelength,  $L_{bp}$  is a pump polarization beat length,  $\alpha_p$  and  $\alpha_s$  are the loss coefficients for pump and signal, respectively.  $\sigma_1$  and  $\sigma_3$  are the corresponding components of the standard Pauli matrix. The last equation in (1) has to be treated as a stochastic differential equation (SDE) of Stratanovich type, where an angle  $\theta$  defines an orientation of birefringence axis and is treated as a stochastic variable with  $\langle \ell(z) \rangle = 0$ ,  $\langle \ell(z)\ell(z') \rangle = \delta(z-z')/L_c$ .

Rotation (C.R. Menyuk and B.S. Marks [5]):

$$|a_{s,p}\rangle = \begin{pmatrix} \cos \frac{\theta}{2} & \sin \frac{\theta}{2} \\ -\sin \frac{\theta}{2} & \cos \frac{\theta}{2} \end{pmatrix} |A_{s,p}\rangle \quad (2)$$

with subsequent transformation:

$$\begin{aligned}|U\rangle &= \Theta|a_s\rangle, |V\rangle = \Theta|a_p\rangle, \\ \Theta &= \begin{pmatrix} \zeta_1 & \zeta_2 \\ -\zeta_2^* & \zeta_1 \end{pmatrix}, |\zeta_1|^2 + |\zeta_2|^2 = 1\end{aligned}\quad (3)$$

split the initial system of SDE (in partial derivatives, in general case) into a set of evolutionary equations for fields:

$$\begin{aligned}\frac{d|U\rangle}{dz} &= \frac{g_R}{2}|V\rangle\langle V|U\rangle - \alpha_s|U\rangle + i\pi\left(\frac{1}{L_{bs}} - \frac{1}{L_{bp}}\right)\tilde{\sigma}_3|U\rangle, \\ \frac{d|V\rangle}{dz} &= \frac{g_R\lambda_s}{2\lambda_p}|U\rangle\langle U|V\rangle - \alpha_p|V\rangle\end{aligned}\quad (4)$$

with stochastic coefficients  $\tilde{\sigma}_3 = \Theta^\dagger \sigma_3 \Theta$  pre-determined by independent SDEs:

$$d\Theta(z) = \begin{pmatrix} \frac{i\pi}{L_{bp}} dz & -d\theta(z) \\ d\theta(z) & -\frac{i\pi}{L_{bp}} dz \end{pmatrix}. \quad (5)$$

The main advantage of the system (4,5) is that SDEs (5) can be solved independently once for an arbitrary PMD,  $L$  and a number of stochastic trajectories. Then, obtained “library” of stochastic coefficients  $\tilde{\sigma}_3$  can be used for the solution of any modification, including time-dependent and Kerr-nonlinear, of Eqs. (4) without a need for a solution of stochastic nonlinear PDEs. That provides unprecedented acceleration of calculations and allows analyzing the real-world long stochastic fiber lasers and amplifiers.

Both Eqs. (4) and Eqs. (5) were solving with the help of Matlab. Especial thoroughness is required for the solution of SDEs (5) where unitarity has to be provided for all  $z$  and stochastic trajectories. Fastest and best convergence was provided by the Weak Order 2 Stochastic Runge-Kutta Method (B. Riadh and H. Querdiane [7]), which for a formal Stratanovich type SDE:

$$X(z) = A(z, X)dz + B(z, X) \circ dW(z) \quad (6)$$

can be written in the form:

$$\begin{aligned} Y_0 &= X_0, U = Y_n + A(Y_n)\delta + B(Y_n)\Delta W_n, U_{\pm} = Y_n + A(Y_n)\delta \pm B(Y_n)\sqrt{\delta} \\ Y_{n+1} &= Y_n + \frac{\delta}{2} [A(U) + A(Y_n)] + \frac{\Delta W_n}{4} [B(U_+) + B(U_-) + 2B(Y_n)] + \\ &+ \frac{((\Delta W_n)^2 - \delta)}{4\sqrt{\delta}} [B(U_+) - B(U_-)], \end{aligned} \quad (7)$$

where  $\delta = z_{n+1} - z_n$ ,  $\Delta W = W(z_{n+1}) - W(z_n)$ ,  $W(z_n)$  is a Wiener process and  $X$ ,  $A$  and  $B$  can be multicomponent. After calculation of the stochastic coefficients from Eq. (5) on the basis of (6,7), Eqs. (4) were solved by the ordinary second-order Runge-Kutta method with an extended step  $\delta$ .

Alternative approaches use the multi-scale averaging techniques and lead to systems of ODEs for averaged field parameters. Let us express the matrix (5) in the form:

$$\tilde{\sigma}_3 = \begin{pmatrix} X_1 & X_4^* \\ X_4 & -X_1 \end{pmatrix}, \quad (8)$$

where  $X_1 = \pi L_{bp}^{-2} - \zeta(z)^2$ ,  $X_2 = -2\pi i \zeta(z)/L_{bp}$ ,  $X_3 = 0$ ,  
 $X_4 = -2\pi i \zeta(z)/L_{bp}$ ,  $X_5 = -(\pi L_{bp}^{-2} + \zeta(z)^2)$  and  $X_6 = i(\pi L_{bp}^{-2} - \zeta(z)^2)$   
 which obeys Eq. (6) with the coefficients  
 $A = (0, -2\pi X_3/L_{bp}, 2\pi X_2/L_{bp}, 0, -2\pi X_6/L_{bp}, 2\pi X_5/L_{bp})^T$  and  
 $B = (2X_2, -2X_1, 0, 2X_5, -2X_4, 0)^T$ . If one assumes the stochastic birefringence as a fast variable and average over it (D. Marcuse *et al.* [8]), applying the Dunkin formula and the Stratanovich generator (B. Øksendal [9]):

$$\frac{d\langle f \rangle}{dz} = \hat{\Gamma}[f(X_k)],$$

$$\hat{\Gamma} = \sum_{k=1}^6 A_k \frac{\partial}{\partial X_k} + \frac{1}{2L_c} \sum_{k=1}^6 \sum_{l=1}^6 \left( B_k B_l + B_l \frac{\partial B_k}{\partial X_l} \frac{\partial}{\partial X_k} \right) \quad (9)$$

after cumbersome calculations, the resulting equations for the evolution of signal and pump Stokes parameters are:

$$\frac{d\langle \bar{S} \rangle}{dz} = \frac{g_R}{2} \left( \langle |\bar{P}| \rangle \langle \bar{S} \rangle + \langle |\bar{S}| \rangle \langle \bar{P} \rangle \right) - \alpha_s \langle \bar{S} \rangle +$$

$$+ \pi \left( L_{bs}^{-1} - L_{bp}^{-1} \right) \begin{pmatrix} 0 \\ -\langle S_3 \rangle \\ \langle S_2 \rangle \end{pmatrix} \exp\left(-\frac{2\pi z}{L_c}\right), \quad (10)$$

$$\frac{d\langle \bar{P} \rangle}{dz} = -\frac{g_R \lambda_s}{2\lambda_p} \left( \langle |\bar{P}| \rangle \langle \bar{S} \rangle + \langle |\bar{S}| \rangle \langle \bar{P} \rangle \right) - \alpha_p \langle \bar{P} \rangle,$$

where the connection between Stokes and Jones parameters is  $\bar{S} = \langle U | \bar{\sigma} | U \rangle$ ,

$\bar{P} = \langle V | \bar{\sigma} | V \rangle$ .  $\bar{\sigma}$  is expressed through Pauli matrixes and unit basis vectors:

$\bar{\sigma} = \sigma_1 \bar{i} + \sigma_2 \bar{j} + \sigma_3 \bar{k}$ . Eq.(9) corresponds to Manakov limit of Eq. (1).

If both stochastic and regular components of birefringence are treated as the fast variables, the multi-scale averaging procedure ignoring pump depletion leads to the sets of ODEs for averaged Stokes parameters and their momentums described in S. Sergeev [10] and S. Sergeev *et al.* [11]:

$$\frac{d\langle s_0 \rangle}{dz'} = \varepsilon_1 \exp(-\varepsilon_2 z') \langle x \rangle, \quad \frac{d\langle x \rangle}{dz'} = \varepsilon_1 \exp(-\varepsilon_2 z') \langle s_0 \rangle - \varepsilon_3 \langle y \rangle,$$

$$\frac{d\langle s_0^2 \rangle}{dz'} = 2\varepsilon_1 \exp(-\varepsilon_2 z') \langle s_0 x \rangle, \quad \frac{d\langle y \rangle}{dz'} = \varepsilon_3 (\langle x \rangle - \langle \tilde{p}_1 \tilde{s}_1 \rangle) - \frac{L}{2L_c} \langle y \rangle,$$

$$\frac{d\langle y^2 \rangle}{dz'} = 2\varepsilon_3 (\langle xy \rangle - \langle y \rangle \langle \tilde{p}_1 \tilde{s}_1 \rangle) - \frac{L}{L_c} (\langle y^2 \rangle - \langle u^2 \rangle), \quad (11)$$

$$\frac{d\langle x^2 \rangle}{dz'} = 2\varepsilon_1 \exp(-\varepsilon_2 z') \langle s_0 x \rangle - 2\varepsilon_3 \langle xy \rangle,$$

$$\frac{d\langle xy \rangle}{dz'} = \varepsilon_1 \exp(-\varepsilon_2 z') \langle s_0 y \rangle + \varepsilon_3 (\langle x^2 \rangle - \langle x \rangle \langle \tilde{p}_1 \tilde{s}_1 \rangle) - \frac{L}{2L_c} \langle xy \rangle,$$

$$\frac{d\langle s_0 y \rangle}{dz'} = \varepsilon_1 \exp(-\varepsilon_2 z') \langle xy \rangle + \varepsilon_3 (\langle s_0 x \rangle - \langle y^2 \rangle - \langle s_0 \rangle \langle \tilde{p}_1 \tilde{s}_1 \rangle) - \frac{L}{2L_c} \langle s_0 y \rangle,$$

$$\frac{d\langle s_0 x \rangle}{dz'} = \varepsilon_1 \exp(-\varepsilon_2 z') \left( \langle s_0^2 \rangle + \langle x_0^2 \rangle \right) - \varepsilon_3 \langle s_0 y \rangle,$$

$$\frac{d\langle u^2 \rangle}{dz'} = \frac{L}{L_c} \left( \langle y^2 \rangle - \langle u^2 \rangle \right),$$

In Eqs. (11)  $z' = z/L$ ,  $\langle x \rangle = \langle \vec{s} \cdot \vec{p} \rangle$ ,  $\langle y \rangle = \langle \tilde{p}_3 \tilde{s}_2 - \tilde{p}_2 \tilde{s}_3 \rangle$ ,  $\langle u \rangle = \langle \tilde{p}_3 \tilde{s}_1 - \tilde{p}_1 \tilde{s}_3 \rangle$ ,  $\langle \tilde{p}_1 \tilde{s}_1 \rangle = \tilde{p}_1(0) \tilde{s}_1(0) \exp(-z'/L_c)$ ,  $\varepsilon_1 = g_R P(0) L/2$ ,  $\varepsilon_2 = \alpha_s L$ ,  $\varepsilon_3 = 2\pi L(\lambda_s/\lambda_p - 1)/L_{bp}$ . The normalization for Stokes vector is used:

$$\vec{S} = s_0 \vec{s} \exp\left(\int_0^L (g_R p_0(z')/2 - \alpha_s z') dz'\right). \quad s_0 = |\vec{S}|, \quad p_0 = |\vec{P}| \quad \text{and} \quad s_k, p_k$$

( $k=1,2,3$ ) are amplitudes and unit vectors describing the orientation of corresponding Stokes vectors, respectively. Tildes mean that the chosen coordinate system corresponds to the reference frame where the birefringence vector oriented along the principal state of polarization on the Poincaré sphere (S. Sergeev *et al.* [11]). We will name this limit (Eqs. (11)) as “diffusion” one.

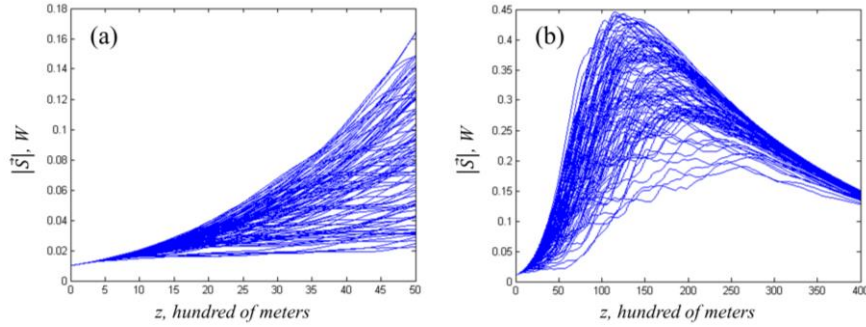


Fig. 1. 1000 stochastic trajectories for the signal power  $|\vec{S}(z)|$  obtained from

Eqs. (4,5) for  $g_R=0.8 \text{ W}^{-1}\text{km}^{-1}$ ,  $|\vec{S}(0)|=10 \text{ mW}$ ,  $|\vec{P}(0)|=1 \text{ W}$ ,  $L_c=100 \text{ m}$ ,

$\alpha_p \approx \alpha_s = 0.2 \text{ dB/km}$ ,  $\vec{S}(0)$  and  $\vec{P}(0)$  are collinear,  $L_{bs}=125 \text{ m}$ ,  $L_{bp} = L_{bs}\lambda_s/\lambda_p$ ,  $L=5 \text{ km}$  (a) and  $40 \text{ km}$  (b).  $D_p=0.026 \text{ ps/km}^{1/2}$  (see Fig. 2).

### 3 Results and Discussion

Fig. 1 demonstrates the 1000 independent stochastic trajectories for the signal powers  $|\vec{S}(z)|$  in dependence on propagation distance for the case of  $L_{bs} \approx L_c$  ( $D_p=0.026 \text{ ps/km}^{1/2}$ ) that satisfies the SAR requirement (V.L. Kalashnikov *et al.* [4]). One can see a substantial wandering and divergence of

trajectories for  $L=5$  km (Fig. 1 (a)). Dispersion of the mean Raman gain  $\langle G \rangle = 10 \log \left( \frac{\langle |\tilde{S}(L)| \rangle}{|\tilde{S}(0)|} \right)$  is defined as  $\sigma = \sqrt{\frac{\langle |\tilde{S}(L)|^2 \rangle}{\langle |\tilde{S}(L)| \rangle^2} - 1}$  and has a sharp maximum near SAR if the fiber length  $L$  is located within diapason  $\approx 5 \div 10$  km (see Fig. 2). It is clear that a trajectory wandering has no sufficient time to develop for smaller propagation lengths. Therefore, the gain dispersion decreases with the  $L$ -decrease (Fig. 2). As is seen from Fig. 2, the maximum of gain dispersion shifts to larger PMD parameters with the  $L$  decrease.

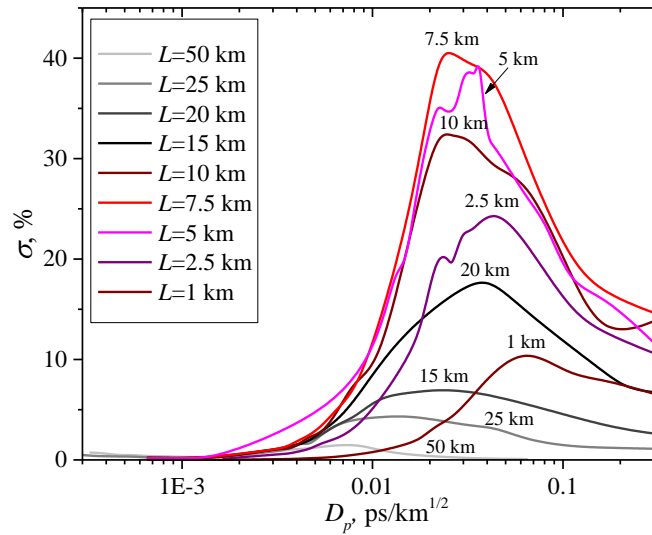


Fig. 2. Dependencies of the relative mean gain dispersions  $\sigma$  on the PMD parameter  $D_p$  for the different fiber lengths  $L$  (inscribed). All other parameters correspond to Fig. 1.

The interesting effect takes place with the propagation length growth (Fig. 1 (b)). In this case, the gain depletion intensifies that decreases the signal power with  $z$  and the SOP pulling “squeezes” an assemblage of trajectories and presses them to some maximum value (see Fig. 1 (b)). Distribution of signal powers at  $L$  changes from a Gaussian-like to extreme-like one with a sharp high-power edge and a stretched low-power tale (Fig. 3, S. Coles [12]). The presence of such low-power trajectories is clearly visible in Fig. 1 (b). A similar behavior takes place for small  $L$  and small  $D_p$  where the SOP pulling is maximum that corresponds to the Manakov limit (see Eqs. (10) and the left side of Fig. 2 with extremely low gain dispersion). PMD corresponding to SAR decreases with the  $L$  growth (Fig. 2).

The Manakov limit obtained from Eqs. (10) in dependence on the fiber length  $L$  is shown in Fig. 4 by the solid curve. As one can see from the first Eq. (10), the contributions of both regular and stochastic birefringence to the evolution of relative pump-signal SOP is suppressed exponentially with distance. It corresponds to the case of a full polarization pulling (trapping). The decrease of the mean gain with distance is a consequence of pump depletion.

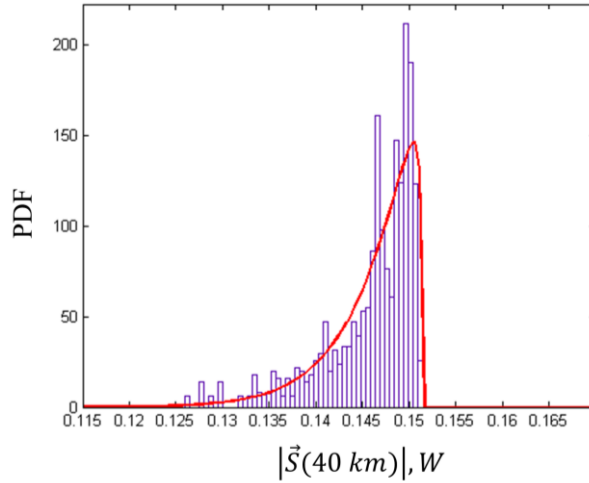


Fig. 3. Probability distribution function (PDF) of signal power for 1000 stochastic trajectories. Fitting red curve corresponds to a generalized extreme PDF.  $D_p=0.026$  ps/km<sup>1/2</sup>,  $L=40$  km. All other parameters correspond to Fig. 1.

Circles and triangles show the results of exact numerical calculations based on Eqs. (4, 5). One can see, that the Monakov limit describes perfectly the situations of long fibers and/or small PMD. Simultaneously, the multi-scale averaging procedure leading to Eqs. (11) gives an exact result for relatively short fibers regardless of PMD value (dotted and dashed curves in Fig. 4). Such a multi-scale averaging technique describes a system in diffusion limit and in the vicinity of SAR (V. Kalashnikov *et al.* [4]). The source of discrepancy between the results of Eqs. (4, 5) and Eqs. (11) for long fibers is an absence of taking into account of pump depletion in the procedure of multi-scale averaging technique.

An important characteristic of a system under consideration is its ability to transfer the pump noise to the signal one (C. Headley and G. P. Agrawal [1]). Fig. 5 demonstrates the dependencies of the mean gain dispersions on the PMD parameters in the absence and in the presence of input pump noise (solid and dashed curves, respectively). One can see, that an input noise contributes mainly in the Manakov limit, that is in a regime of SOP pulling, enhancing the signal SOP noise substantially. Such an enhancement can even growth with the further PMD decrease. This conclusion is supported by the character of the behavior of the integral pump-noise transfer function (C.

Headley and G. P. Agrawal [1]):  $H_{\text{int}} = 10 \log(\sigma_G^2 / \sigma_P^2)$ . The dependence of this value on  $D_p$  is shown in Fig. 5 by filled circles connected by a dotted curve. One can see, that the maximum pump-noise transfer corresponds to SAR, but it does not vanish with the PMD decrease and can even grow in the Manakov limit.

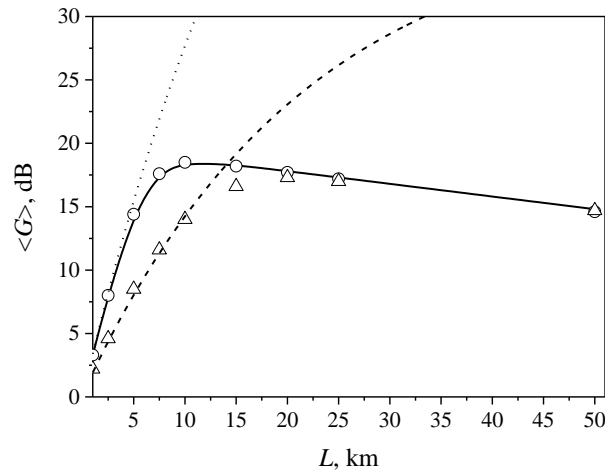


Fig. 4. Mean gain  $\langle G \rangle$  vs. fiber length  $L$  in the Monakov limit (solid curve) from Eqs. (10) and from Eqs. (4, 5) ( $D_p=0.001 \text{ ps/km}^{1/2}$  for circles and  $0.065 \text{ ps/km}^{1/2}$  for triangles). Dotted and dashed curves are obtained from the multi-scale averaging procedure leading to Eqs. (11) and correspond to  $D_p=0.001 \text{ ps/km}^{1/2}$  and  $0.065 \text{ ps/km}^{1/2}$ , respectively.

## Conclusions

We analyzed a fiber Raman amplifier in the presence of the stochastic birefringence and the pump depletion. The analysis was based on two approaches, namely the exact numerical solution of SDEs in the Jones and Stokes representations and the techniques of averaging over fast variables. The last approach was realized by two ways, that are i) averaging over stochastic birefringence as a fast variable, and ii) averaging over both stochastic birefringence and regular SOP beating as fast variables. It was found, that SAR, i.e. resonance-like enhancement of mean gain fluctuations within confined region of PMD, exists within bounded domain of fiber lengths and is suppressed for both short fibers (that is so-called diffusion limit where SAR has not time to develop) and long ones (that is so-called Manakov limit where SAR is suppressed by strong SOP pulling). Comparison of the numerical results with the results based on averaging techniques shown that the approach (i) gives an excellent agreement with the exact numerical solution of Eqs. (4, 5) in the

Manakov limit, that is for long fibers and/or small PMD. Approach (ii) is valid for arbitrary PMD in diffusion limit, i.e. for relatively short fibers. One has to note, that deviation of the results of approach (ii) from the exact numerical ones for long fibers is caused by the absence of pump depletion in Eqs. (11). Taking into account of a pump depletion in the frameworks of this approach is a goal of further analysis. Additionally, the pump-signal noise transfer was analyzed. It was found, that a stochastic behavior near SAR is defined mainly by the stochastic birefringence, but the pump-signal noise transfer is maximum here, as well. Simultaneously, such a transfer does not vanish and can even grow with the PMD decrease, i.e. in the Manakov limit. This effect can be explained by a strong coupling of pump and signal SOPs (polarization pulling).

The outlook for further analysis can be characterized in the following way. The presented numerical technique splitting the initial combined system of SDEs into two subsystems of the ODEs with the *pre-defined* stochastic coefficients for fields and the *independent* SDEs for a fiber allows generalizing on the case when group-delay, its dispersion, and Kerr nonlinearity are taken into account, i.e. on a system of PDEs with fixed stochastic coefficients.

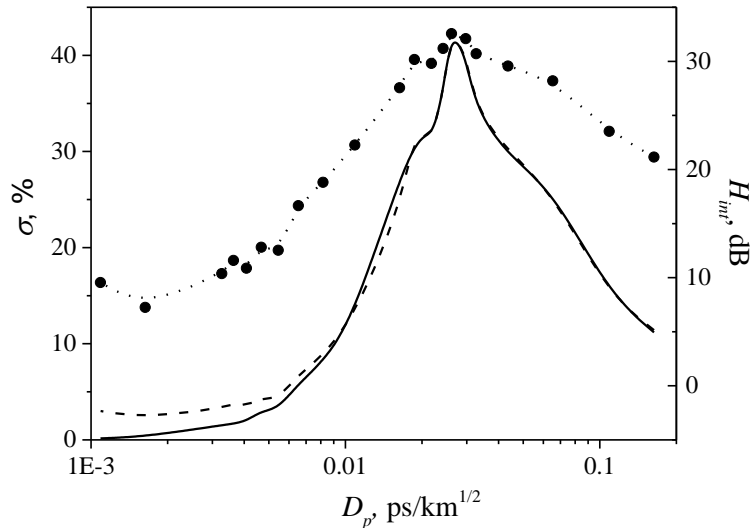


Fig. 5. Dispersion  $\sigma$  in absence and in the presence of pump noise (solid and dashed curves, respectively) and integral pump-noise transfer function  $H_{int}$  (filled circles connected by dotted curve) vs. PMD parameter  $D_p$ . Power pump fluctuations are Gaussian with 1% standard deviation.  $L=5$  km. Other parameters correspond to Fig. 1.

## Supplementary materials

“Stochastic Anti-Resonance in a Fibre Raman Amplifier” on <http://info.tuwien.ac.at/kalashnikov/programs.html>

## Acknowledgments

This work was supported by the FP7-PEAPPLE-2012-IAPP project GRIFFON (No. 324391) and the Austrian Science Fund (FWF project P24916-N27).

## References

1. C. Headley and G. P. Agrawal, Eds. Raman Amplification in Fiber Optical Communication Systems, Elsevier, Amsterdam, 2005.
2. A. Galtarossa, C.R. Menyuk. Polarization Mode Dispersion, Springer, New-York, 2005.
3. V.V. Kozlov, J. Nuño, J.D. Ania-Castañón, S. Wabnitz. Trapping polarization of light in nonlinear optical fibers: an ideal Raman polarizer, in Spontaneous Symmetry Breaking, Self-Trapping, and Josephson Oscillations. B.A. Malomed, Ed. Progress in Optical Science and Photonics, pp. 227–246, Springer, Berlin, 2013.
4. V. Kalashnikov, S.V. Sergeev, G. Jacobsen, S. Popov, Multi-scale polarisation phenomena. Nature, Light: Science & Applications, 5, e16011, 2016.
5. C. R. Menyuk, B. S. Marks. Interaction of polarization mode dispersion and nonlinearity in optical fiber transmission systems. J. Lightwave Technol., 24, 2806, 2006.
6. V.L. Kalashnikov, S.V. Sergeev, Stochastic Anti-Resonance in Polarization Phenomena, in The Foundations of Chaos Revisited: From Poincaré to Recent Advancements. Ch. Skiadas Ed., pp. 159-179, Springer, 2016.
7. B. Riadh, H. Querdiane. A comparative study of numerical simulation of stochastic differential equations. Application to stochastic Duffing-oscillator. Int. J. Math. Analysis, 8, 229, 2014.
8. D. Marcuse, C. R. Menyuk, P.K.A. Wai. Application of the Manakov-PMD equation to studies of signal propagation in optical fibers with randomly varying birefringence. IEEE J. Lightwave Technology, 15, 1735, 1997.
9. B. Øksendal. *Stochastic Differential Equations* (Berlin, Springer, 2007).
10. S. Sergeev. Activated polarization pulling and de-correlation of signal and pump states of polarization in a fiber Raman amplifier. Opt. Express, 19, 24268, 2011.
11. S. Sergeev, S. Popov, and A. T. Friberg. Virtually isotropic transmission media with fiber Raman amplifier. IEEE J. Quantum Electron., QE-46, 1492, 2010.
12. S. Coles. An Introduction to Statistical Modeling of Extreme Values, Springer, London, 2001.